Influence of the Processing Parameters on the Electrospinning of Biopolymeric Fibers

Alicia Mujica-Garcia[1,2], Iván Navarro-Baena[1], José Maria Kenny[1,2] and Laura Peponi*[,2]

[1]*Department of Civil and Environmental Engineering, University of Perugia, Terni, Italy*
[2]*Institute of Polymer Science and Technology, ICTP, of the Spanish Council for Scientific Research, CSIC, Madrid, Spain*

Received December 16, 2013; Accepted February 02, 2014

ABSTRACT: The main aim of this research is the production of different biopolymeric fibers by electrospinning and the determination of the optimum working parameters for each polymer analyzed. In particular, three different biopolymers have been studied: poly(lactic acid) (PLA), poly(ε-caprolactone) (PCL) and a synthesized poly(ester-urethane) based on a synthesized PLA-b-PCL-b-PLA tri-block copolymer. This research is focused on the analysis of the influence of the processing parameters, such as the concentration and flow-rate of the polymer solution and the applied voltage, as well as the physico-chemical properties of the polymers used, on the fiber formation and crystallization behavior. Therefore, the optimum working conditions for each polymer were determined and related to the final properties of the electrospun fibers in terms of geometry, homogeneous morphology and crystallinity.

KEYWORDS: PLA, PCL, crystallization, electrospinning, poly(ester-urethane), polymeric fiber

1 INTRODUCTION

In recent years, eco-friendly products have generated great interest for packaging and biomedical applications, among other applications. In this regard, some of these promising materials are represented by biopolymers as an alternative to oil-derived materials. In fact, it is possible to reduce the environmental impact by using biopolymeric materials such as poly(lactic acid) (PLA). Poly(lactic acid) is a thermoplastic biodegradable polyester obtained from renewable resources, with a glass transition temperature at about 60°C and a melting temperature around 160°C, indicating its suitable processability [1, 2]. It is used in biomedical and packaging applications due to its high biocompatibility and biodegradability [3]. However, its application is still limited, due to its fragility and its low thermal stability [2].

Among biopolymers, poly(ε-caprolactone) (PCL) also plays an important role. Poly(ε-caprolactone) has a low melting temperature of about 60°C and its glass transition temperature is around −60°C. It presents good mechanical and biodegradable properties [4]. In general, PCL is used in drug delivery applications, while its hydrophilic and biocompatibility properties can be improved by blending [5] or copolymerizing it with other polymers [6] and, above all, with PLA [7–9]. In particular, from the copolymerization of PCL and PLA it is possible to obtain poly(ester-urethane)s (PUs) [2, 10] with good mechanical properties and biocompatibility [11].

Thermoset and thermoplastic poly(urethane)s are obtained by polycondensation. They can be used as foams, rigid materials, films, adhesives, coatings and also for biomedical applications [12–14].

Biopolymers can be processed to obtain polymeric fibers by two common processes with different driving forces, the conventional mechanical spinning process and electrospinning. In the conventional mechanical spinning process, a mechanical force is applied by a rotating mandrel to the fluid, which is transformed in hydraulic pressure that pushes the forming jet [15]. Besides, in the electrospinning process, volumetric electrical forces are applied to the charged jet [16]. Moreover, the electrospinning process can be carried out from polymer solutions or polymer melts. In the

**Corresponding author*: lpeponi@ictp.csic.es

DOI: 10.7569/JRM.2013.634130

first case, rapid solvent evaporation determines the size, the structure and the morphology of the electrospun fibers. In the case of polymer melts, the rapid solidification during drawing determines the final properties of the fibers [15, 16]. The electrospinning process based on polymer solution can be considered the best method in order to obtain polymeric nanofibers compared with the melt electrospinning process [17–19]. A more detailed explanation of the process follows.

In the electrospinning process based on polymer solution, a voltage is applied between the tip and the collector. Charges accumulated in the tip cause the formation and elongation of polymer solution drops. Generally, electric forces must be higher than cohesion forces of the polymer solution related to its surface tension. When voltage increases, the drop is elongated, thus reaching a conic form called the Taylor cone [20]. When the Taylor cone is stable, the charged polymeric solution is attracted towards the collector and the jet gets narrower due to the elongation as well as the solvent evaporation. So, the electrospun fibers are obtained and they can be collected in the form of single fibers as well as random or oriented mats [21, 22]. Electrospun bio-nanofibers can be used in a wide range of applications mainly in the biomedical field, as sutures, drug delivery systems or tissue engineering scaffolds [23].

In order to obtain suitable electrospun fibers, different parameters have to be optimized. Parameters related to the polymeric solution include polymer molecular weight, concentration, viscosity, conductivity and surface tension, and those related to the proper processing conditions include the flow rate, the applied voltage, the working distance between the tip and the collector and even the atmospheric conditions [23–28].

Some research on the electrospinning of biopolymers has been reported in previous years. In particular, the electrospinning of PLA has been studied by Zhou *et al.* [21], Mei *et al.* [16] and Sonseca *et al.* [22], analyzing their morphologies and thermal properties. The electrospinning of PCL fibers was reported by Li *et al.* [6] and Liao *et al.* [11], studying their application in tissue engineering and drug release. Polyurethane (PU) electrospun fibers were obtained by Pedicini *et al.* [12] and Khil *et al.* [13], with attention focused on their mechanical and tissue engineering applications.

In this work, we focus the attention on the electrospinning process of different biopolymer solutions. In particular, PLA, PCL and PU have been chosen as biopolymers in order to study the optimization of both classes of parameters, those related to the physicochemical properties of the polymers and those due to the electrospinning process. Moreover, taking into account that the PU is synthesized starting from PLA-b-PCL-b-PLA tri-block copolymer, firstly, a deep study on the electrospinning capability of PLA as well as of PCL have been carried out.

Finally, the thermal properties of the biopolymer electrospun fibers obtained for each biopolymer are compared with the respective solvent-casting biopolymeric films in order to study the effect of the electrospinning process on the crystallization of the electrospun fibers.

2 EXPERIMENTAL

2.1 Materials

Two different Poly(lactic acid), PLA 3051D and PLA 2003D, were supplied by NatureWorks® (USA). The PLA 3051D has a molecular weight of 11×10^4 g/mol and 3% D-lactic acid monomer, while PLA 2003D has a molecular weight of 12×10^4 g/mol and 4.25% D-lactic monomer. Poly(ε-caprolactone) (PCL) was supplied by Perstorp (Sweden) with 0.5% of ε-caprolactone monomer and its molecular weight is 5×10^4 g/mol.

L-lactide (L-LA), ε-caprolactone (ε-CL), hexamethylene diisocyanate (HDI) and the catalyst tin(II) 2-ethylhexanoate ($Sn(Oct)_2$) were purchased from Sigma Aldrich. The PCL-diol CAPA 2803, kindly donated by Perstorp, has a molecular weight of 4021 g/mol. Chloroform and dimethylformamide (DMF) purchased from Sigma Aldrich, with solubility parameters of 19 $J^{1/2}/cm^{3/2}$ and 24.9 $J^{1/2}/cm^{3/2}$, respectively, were used as solvents; no demixing was observed in the mixture of both solvents during processing. All the materials were used without further purification.

2.2 Synthesis of Poly(ester-urethane)

Poly(ester-urethane) was synthesized in two steps following a procedure detailed elsewhere [10]. Ring-opening polymerization of L-lactide in bulk was carried out initiated by PCL-diol, obtaining a tri-block copolymer with a weight ratio of 50:50 between two blocks. $Sn(Oct)_2$ was employed as catalyst at 0.1% (wt) with respect to the amount of LA monomer. The reaction took place in a round-bottom flask, previously dried, using an oil bath at 180°C for 3 h. When the reaction finished, after cooling, the tri-block copolymer was dissolved in chloroform. Next, it was precipitated using cold methanol, separated by filtration and dried under vacuum for 24 h.

In the second step, the tri-block copolymer and 1,6-hexamethylene diisocyanate (HDI) reacted with a molar ratio of 1:1 at 80°C for 5 h using $Sn(Oct)_2$ as catalyst, obtaining the poly(ester-urethane) in 2,2-dichloroethane. The PU obtained was cast in a leveled glass

covered with a conical funnel to remove the solvent at room temperature for 24 h. At the end, the polymeric film was dried under vacuum for 24 h to remove traces of solvent [10].

2.3 Production of Nanofibers by Electrospinning

Electrospun polymeric fibers were prepared using an Electrospinner Yflow 2.2.D-XXX with a vertical standard configuration with two concentric needles; the polymer solution flows through the inner needle and the solvent flows through the outer one. Solvents used in the outer needle to obtain fibers were the same used for the polymeric solutions.

Following an extensive experimental campaign a mixture of solvents was chosen for all the polymers studied (chloroform-DMF 4:1). Both systems (polymer solution and solvent mixture) were loaded into the syringes and flow-rates were set and stabilized. Then, an electric voltage, using a voltage DC supply, was applied between the jet and the collector where electrospun fibers were deposited [20].

Due to the technical characteristics of our electrospinning machine we can regulate the applied difference of potential by varying both positive and negative applied voltages; the positive voltage applied on the jet and the negative one applied on the collector.

The experimental strategy used to obtain the electrospun fibers in terms of materials, number of samples tested and processing parameters, is summarized in Table 1. The samples which were analyzed in order to find the optimum working conditions are named Sx, where x corresponds to the number of the sample and are detailed in the tables reported below in the Results and Discussion section.

2.4 Characterization Methods

The molecular weight of the tri-block polymers obtained during the first step of the poly(ester-urethane) synthesis was calculated using proton nuclear magnetic resonance (1H-NMR). The NMR spectra were obtained at room temperature in a Varian Unity Plus 400 instrument using deuterated chloroform ($CHCl_3$) as solvent and were referenced to the residual solvent protons at 7.26 ppm. The average molecular weights and polydispersity were determined by gel permeation chromatography (GPC) using a refractomer index detector Waters 2414. For the determination of the molecular weight, the samples were referenced to polystyrene standards between 4×10^3 and 4×10^5 g/mol.

Differential scanning calorimetry (DSC) analysis was performed in a Mettler Toledo DSC822e instrument. Samples of about 10 mg were sealed in aluminium pans. Thermal cycles composed by two heating scans (25–200°C and −90–200°C, respectively) with a cooling scan (200– −90°C) in between were performed with a heating rate of 10°C/min under nitrogen purge. The melting points (T_m) and the crystallization temperatures (T_c) were taken as the maximum and minimum of the endothermic and exothermic transitions, respectively. Glass transition temperatures (T_g) have been calculated from the second heating scan, while the crystallinity was determined from the first scan, using the following equation:

$$X_c = \frac{\Delta H_f}{\Delta H_{f,100\%}} \cdot 100 \quad (1)$$

where ΔH_f is the melting enthalpy measured from the thermogram peak and $\Delta H_{f,100}$ is the theoretical melting enthalpy for a 100% crystallized polymer. Values of $\Delta H_{f,100}$ for PCL and PLA were taken from previous reports as 148 J/g [29] and 93 J/g [30] respectively. Also, the weight fraction of each polymer was considered in the calculation of the crystallinity in the case of the PU [10].

Electrospun fibers' morphology and structure were observed using a Scanning Electron Microscope (SEM) PHILIPS XL30. Previously, a layer of gold/ palladium

Table 1 Main range of the experimental conditions used during the electrospinning process for PLA, PCL and PU in terms of concentration (C (% (wt)), solvent flow-rate (Q_S (mL/h)), polymer solution flow-rate (Q_P (mL/h)) and positive and negative applied voltages (V^+, V^-)). The first number indicates the number of values taken in the interval indicated between brackets.

Polymer	Number of samples	Concentration C (% (wt))	Solvent flow rate Q_S (mL/h)	Polymer flow rate Q_P (mL/h)	Positive Voltage V^+	Negative Voltage V^-
PLA	30	2 (8–10%)	9 (0.1–3.5)	10 (0.1–7)	12 (2.0–11.4)	12 (0.4–10.5)
PCL	17	2 (8–10%)	5 (0.1–2)	6 (0.1–5)	9 (1.5–9.8)	9 (3.0–9.8)
PU	99	4 (12–35%)	7 (0.1–3.5)	7 (0.1–7)	11 (2.0–9.8)	11 (0.4–9.8)

was deposited on the samples employing Polaron SC7640 equipment. Fiber diameters have been statistically calculated from the SEM images by using the Fib_thick software, which is executable under image analysis platform Fiji based on ImageJ.

3 RESULTS AND DISCUSSION

When working with electrospinning two main parameter classes must be considered: those related to the polymer solution and those related to the processing conditions. In this research, both parameter classes have been varied and correlated with the morphology of the final electrospun fibers.

However, considering the numerous variables involved, we preferred to adopt a "one factor at a time" method in order to find the optimum working conditions for each biopolymer. So, firstly, the morphologies of the fibers were correlated to the polymer concentration in the starting solutions. Then, once the optimum concentration for each biopolymer was chosen, the best conditions for the flow-rate were studied. Once these variables were fixed, then the applied voltage was studied. In order to obtain the best working conditions for each variable, the diameters as well as the morphologies of the electrospun fibers were analyzed. Table 1 reports the main range of the experimental conditions employed to obtain PLA, PCL and PU electrospun fibers in terms of concentration (C % (wt)), solvent flow-rate (Q_S (mL/h)), polymer solution flow-rate (Q_P (mL/h)) and positive and negative applied voltages (V^+, V^-). In particular, 30 samples for PLA have been studied, as well as 17 for PCL and 99 for PU, as shown in Table 1.

Many more experiments than those reported in Table 1 were performed. In fact, the scope of this work was to find the optimum working conditions for each polymer, so, for example, all the 17 experimental conditions for the PCL are summarized in Table 2, named PCLx, where x varies from 1 to 17.

3.1 Morphology and Size of PLA, PCL and PU Electrospun Fibers

The influence of the polymer solution concentration on the morphology of the electrospun biopolymeric fibers was analyzed. For all the polymers a mixture of solvents of chloroform:DMF at 4:1 was chosen as a result of a preliminary study confirming that this solvent mixture allows obtaining suitable PCL and PLA nanofibers, as indicated in Figure 1 for PLA 2003D and in Figure 2 for PLA 3051D (similar results not shown here were obtained for PCL).

Moreover, based on this preliminary study, we found that PLA 3051D shows better results in terms of electrospinning processing viability compared with

Table 2 PCL samples analyzed.

Polymer	C (% (wt))	Q_S (mL/h)	Q_P (mL/h)	V^+	V^-	Fiber diameter (μm)
PCL1	8%	0.2	0.5	1.5	–8.4	No fiber formation
PCL2	8%	0.2	0.5	2.1	–7.9	No fiber formation
PCL3	8%	0.2	0.5	5.2	–5.5	No fiber formation
PCL4	8%	1.0	2.0	2.1	–7.9	No fiber formation
PCL5	8%	1.0	2.0	4.2	–6.0	No fiber formation
PCL6	8%	1.0	2.0	5.2	–5.5	No fiber formation
PCL7	8%	1.0	4.0	5.2	–5.5	No fiber formation
PCL8	10%	0.1	0.1	4.9	–4.7	0.19 ± 0.02
PCL9	10%	0.2	0.5	3.0	–7.4	No fiber formation
PCL10	10%	0.2	0.5	4.9	–4.7	No fiber formation
PCL11	10%	0.2	0.5	7.4	–3.0	No fiber formation
PCL12	10%	0.3	0.6	3.0	–7.4	No fiber formation
PCL13	10%	0.3	0.6	4.9	–4.7	0.52 ± 0.03
PCL14	10%	0.3	0.6	7.4	–3.0	No fiber formation
PCL15	10%	0.3	0.6	9.8	–9.8	0.47 ± 0.04
PCL16	10%	0.3	2.0	6.3	–8.0	0.23 ± 0.02
PCL17	10%	2.0	5.0	4.9	–4.7	No fiber formation

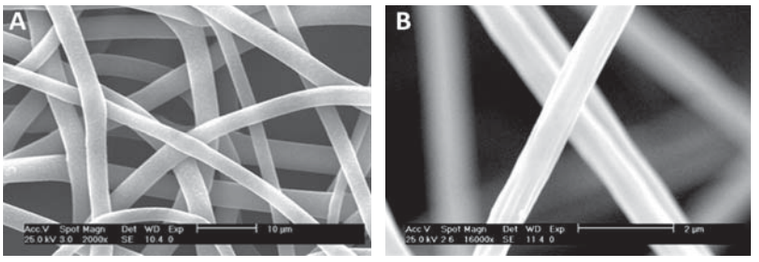

Figure 1 SEM images of PLA 2003D electrospun fibers obtained from 10% (wt) PLA solutions employing a voltage difference of 21 kV and polymer and solvent flow-rates of 0.3 mL/h using **A**) $CHCl_3$ and **B**) $CHCl_3$:DMF 4:1.

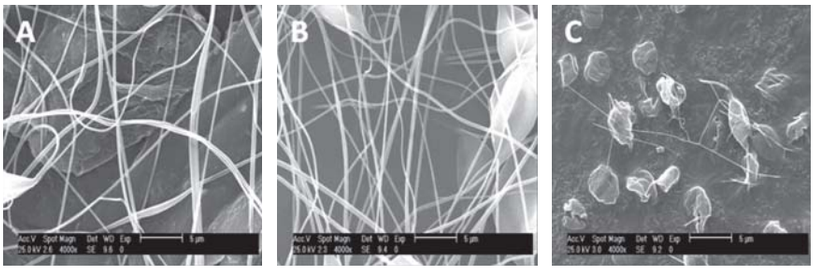

Figure 2 SEM images of PLA 3051D electrospun fibers obtained from 7% (wt) PLA solutions applying a voltage difference of 21 kV and polymer and solvent flow-rates of 0.3 mL/h using **A**) $CHCl_3$:DMF 4:1, **B**) $CHCl_3$:DMF 3:1 and **C**) $CHCl_3$:DMF 2:1.

PLA 2003D, so for further analysis in this work we report only the study related to the PLA 3051D . First, the effects of the polymer concentration on the morphology of PLA electrospun fibers were analyzed. In particular, solutions with 8% (wt) (S1) and 10% (wt) (S2) in the solvent mixture chloroform-DMF 4:1 were studied varying the process parameters in order to find their optimum working conditions [Table 3].

SEM images for the fibers obtained for the S1 and S2 samples are shown in Figure 3a and 3b, respectively. It is worth noting that the formation of beads at the lower concentration is due to the lower solution viscosity leading to lower surface tension and viscoelastic forces that cannot balance the electrostatic forces. Then, electrospun fibers with non-uniform cylindrical morphologies were obtained. Average fiber diameters were obtained for S1 (0.50 ± 0.05 µm) and S2 (2.03 ± 0.22 µm) from the size distributions. Therefore, when the concentration was increased, higher fiber diameters were obtained. So, the concentration of 8% (wt) for the PLA in the chloroform:DMF 4:1 solvent mixture was chosen for further analysis.

Also, in the case of PCL, solutions of 8 and 10% (wt) in the solvent mixture chloroform:DMF 4:1 were prepared in order to obtain electrospun nanofibers. No fibers were obtained from the PCL 8% (wt) solution even if a wide range of flow-rates and electric voltages was analyzed. This fact is due to the low surface tension, which produces fibers which break into drops before being deposited on the collector. On the other hand, good fibers with average diameter 0.52 ± 0.03 µm were obtained for the sample S3 with 10% (wt) of PCL. So, for further analysis a 10% (wt) of PCL solution was used as optimum concentration.

In order to establish the influence of the flow-rates on the final properties of the PLA electrospun fibers, many conditions [see Table 1] were tested on the 8% (wt) PLA solution in the chloroform-DMF 4:1 solvent mixture. The electrospinning conditions used to determinate the specific influence of the flow-rates are summarized in Table 4.

Figure 4 shows SEM images of PLA electrospun fibers of the samples S4 (Figure 4a) and S5 (Figure 4b) obtain with a flow rate of 0.8 mL/h for both the polymer solution and the solvent respectively. In both cases, bead-free electrospun nanofibers were obtained. Moreover, following Table 3 results, an increase of the fiber diameter with the flow-rate is observed, obtaining an average fiber diameter of 0.89 ± 0.09 µm for S4 and of 1.05 ± 0.07 µm for S5. So, in the further analysis of the 8% (wt) PLA solution, a flow-rate of 0.3 mL/h is considered as optimum processing condition.

In the case of PCL electrospun nanofibers at 10% (wt) in chloroform-DMF 4:1solvent mixture, different values for both polymer and solvent solution

Table 3 Electrospinning conditions for PLA (S1 and S2) and PCL (S3) employed to determinate the influence of the concentration.

Polymer	C (% (wt))	Q_S (mL/h)	Q_P (mL/h)	V^+	V^-	Fiber diameter (μm)
PLA-S1	8%	0.3	2.0	6.3	–8.0	0.50 ± 0.05
PLA-S2	10%	0.3	2.0	6.3	–8.0	2.03 ± 0.22
PCL-S3	10%	0.3	0.6	4.9	–4.7	0.52 ± 0.03

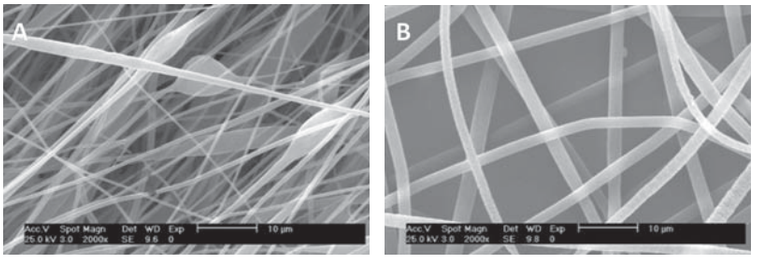

Figure 3 SEM images of PLA electrospun fibers obtained for **A**) 8% (wt) (S1) and **B**) 10% (wt) (S2).

Table 4 Electrospinning conditions for PLA (S4 and S5) and PCL (S3 and S7) used to determinate the influence of the flow-rates.

Polymer	C (% (wt))	Q_S (mL/h)	Q_P (mL/h)	V^+	V^-	Fiber diameter (μm)
PLA-S4	8%	0.3	0.3	10.6	–10.5	0.89 ± 0.09
PLA-S5		0.8	0.8	10.6	–10.5	1.05 ± 0.07
PCL-S3	10%	0.3	0.6	4.9	–4.6	0.52 ± 0.03
PCL-S7		2.0	5.0	4.9	–4.6	No fiber formation

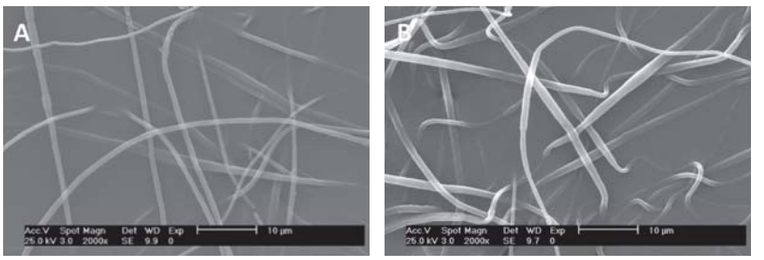

Figure 4 SEM images of PLA electrospun fibers obtained by using both polymer and solvent flow-rates of **A**) 0.3 mL/h (S4) and **B**) 0.8 mL/h (S5).

flow-rates were studied [see Table 1 and Table 4]. The SEM images of both S3 and S7 are shown in Figure 5. It is worth noting that when high flow-rates are used (Figure 5b) many polymer drops are formed and collected, avoiding the formation of polymeric fibers. This fact can be explained by taking into account the force balance and the residence time. Due to the very high flow-rates applied the flowing time is too short, the fiber does not have time to be formed and the gravity effects on the drop are stronger than the electrostatic forces. So, the polymer solution cannot flow constantly and, consequently, electrospun fiber formation is not

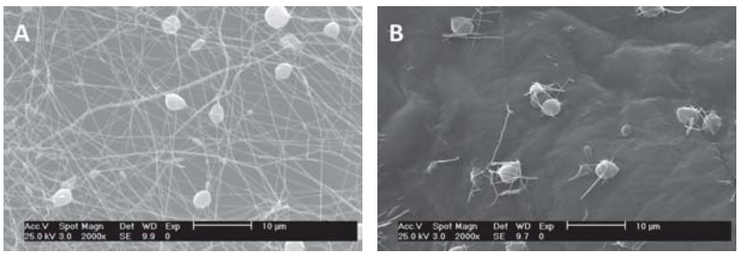

Figure 5 Figure 5 SEM images of PCL electrospun fibers employing **A**) a solvent flow-rate of 0.3 mL/h and polymer solution flow-rate of 0.6 mL/h (S3), and **B**) a solvent flow-rate of 2.0 mL/h and polymer solution flow-rate of 5.0 mL/h (S7).

Table 5 Electrospinning conditions for PLA (S8, S9 and S10) and PCL (S11, S12 and S13) used to determinate the influence of the voltage.

Polymer	C (% (wt))	Q_S (mL/h)	Q_p (mL/h)	V^+	V^-	Fiber diameter (μm)
PLA-S8				10.6	–10.5	0.89 ± 0.09
PLA-S9	8%	0.3	0.3	6.4	–0.5	No fiber formation
PLA-S10				3.0	–7.4	No fiber formation
PCL-S11				3.0	–7.4	No fiber formation
PCL-S12	10%	0.3	0.6	7.4	–3.0	No fiber formation
PCL-S13				9.8	–9.8	0.47 ± 0.04

favored. This also implies that for PCL the optimum conditions regard the application of small flow-rates.

Finally, the influence of the variation of the applied voltage on both PLA and PCL biopolymer systems was studied and is summarized in Table 5 in terms of positive and negative applied voltages as well as the obtained electrospun fiber diameters. In particular, the average electrospun fiber diameters for PLA (S8) and PCL (S13) fibers were calculated from the SEM images reported in Figure 6.

For both biopolymers, high values of applied voltage, both positive and negative, generate the best conditions for the electrospun fiber formation, thus indicating that when the Coulomb forces are increased the elongation of the polymeric drops are favored.

Finally, PU electrospun fibers have been studied. First of all, it is important to underscore that the synthesized PU has a molecular weight of about 26000 g/mol, much lower than the commercial PLA and PCL ones. So, we expect that this difference strongly affects the electrospinning process.

In order to establish the optimum concentration for the production of the PU electrospun fibers, solutions of 12% (wt) (S14), 20% (wt) (S15), 25% (wt) (S16) and 35% (wt) (S17) were prepared in the same chloroform-DMF 4:1 solvent mixture. The electrospinning parameters, the flow-rates and the applied voltage were varied [see Table 6].

Figure 7 shows SEM images of PU electrospun fibers obtained at different polymer concentrations. In particular, fibers were not obtained when employing a solution of 12% (wt). The formation of fibers with a PU solution of 20% (wt) was sporadic (Figure 7a) due to the low polymer solution viscosity; also, in this case the fibers broke into drops before their deposition on the collector. Therefore, this concentration can be considered the lower limit at which PU electrospun fibers can be obtained. At concentrations of 25 and 35% (wt), PU electrospun fibers were obtained (Figure 7b and 7c respectively). Unfortunately, in both cases, beads appeared along the PU electrospun fibers.

In general, beads can be avoided by employing higher solution concentration, and also by increasing the viscosity. In our case, when the polymer concentration was increased above 35% (wt), the solution hardly flowed through the electrospinner needle, leading to flow-rate fluctuations and the formation of beads (Figure 7). Also, for PU, the fiber diameter increases with the polymer concentration. Polymer solution concentrations of 25% (wt) and 35% (wt) were used in order to optimize the processing parameters for the

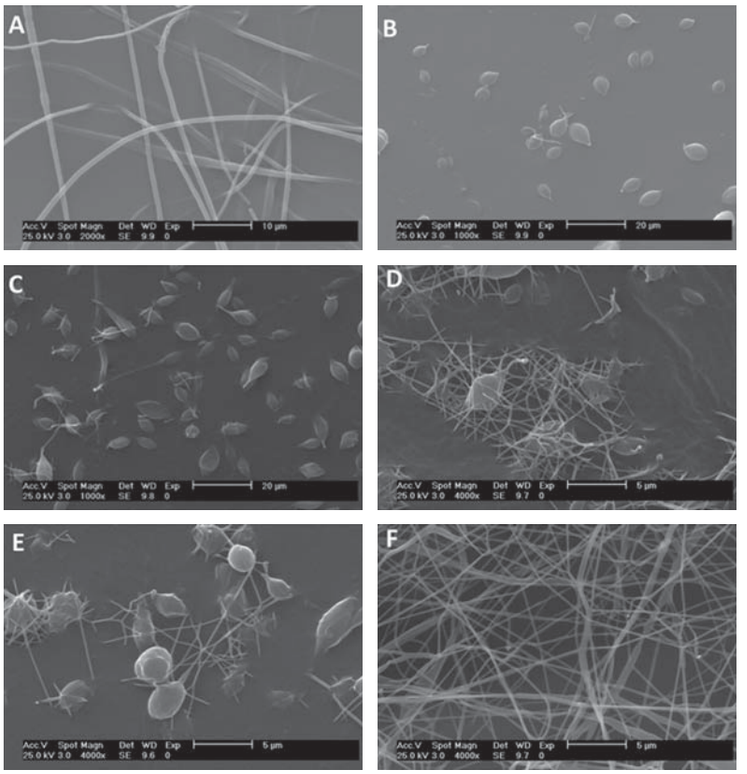

Figure 6 SEM images of electrospun fibers obtained with different applied voltages. PLA: **A**) S8, **B**) S9, **C**) S10 and PCL: **D**) S11, **E**) S12, **F**) S13.

Table 6 Electrospinning conditions for PU (S14, S15, S16 and S17) employed to determinate the influence of the concentration.

Polymer	C (% (wt))	Q_S (mL/h)	Q_P (mL/h)	V^+	V^-	Fiber diameter (μm)
PU-S14	12	0.3	2.0	6.2	–8.0	No fiber formation
PU-S15	20					0.61 ± 0.16
PU-S16	25					0.44 ± 0.02
PU-S17	35					0.54 ± 0.03

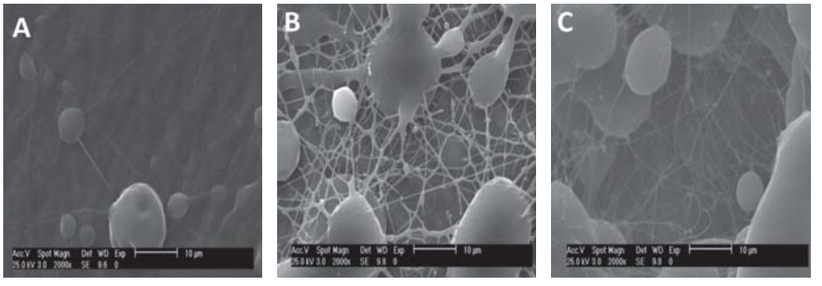

Figure 7 SEM images of PU electrospun fibers obtained from **A**) 20% (wt) (S15), **B**) 25% (wt) (S16) and **C**) 35% (wt) (S17).

PU electrospun fibers, thus varying the flow-rates and the applied voltage.

In order to summarize the influence of the polymer flow-rate on the electrospun fiber diameters, the diameters for PU solutions at 25% and 35% (wt) have been measured as a function of the flow-rate. Table 7 summarizes the different experimental conditions used, as well as the fiber diameters calculated from the SEM images of the samples reported in Figure 8.

It is very difficult to find the optimum condition for the processing of PU electrospun fibers due to the fact that beads are obtained at each experimental condition in the range analyzed.

As discussed before, the low PU molecular weight, of about 26000 g/mol, strongly influenced the final electrospun fibers morphology. So, in future work, the synthesis of PU with higher molecular weight and its influence on the electrospinning process parameters will be analyzed.

3.2 Thermal Characterization of PLA, PCL and PU Electrospun Fibers

The thermal behavior of electrospun fiber samples S2 (PLA), S13 (PCL) and S16 (PU), whose processing conditions were reported before, was studied and the results compared with solvent-casting films obtained from the same polymer solutions.

In order to study how the electrospinning process can affect the crystallinity for each polymer in the electrospun fiber and in the solvent-casting film, DSC thermograms corresponding to the first heating scan were obtained and displayed in Figure 9, while the experimental results in terms of melting temperature, Tg, enthalpy of fusion and crystallinity degree are reported in Table 8.

In particular, there are two main aspects that can affect the crystallization when working with the electrospinning process. On one side, the rapid evaporation

Table 7 Electrospinning conditions for PU (S16, S17, S18 and S19) used to determine the optimum conditions.

Polymer	C (% (wt))	Q_S (mL/h)	Q_P (mL/h)	V^+	V^-	Fiber diameter (μm)
PU-S16	25	0.3	2.0	6.3	–8.0	0.44 ± 0.02
PU-S17	35					0.54 ± 0.03
PU-S18	25	0.3	0.6	9.8	–9.8	0.41 ± 0.03
PU-S19	35					1.97 ± 0.07

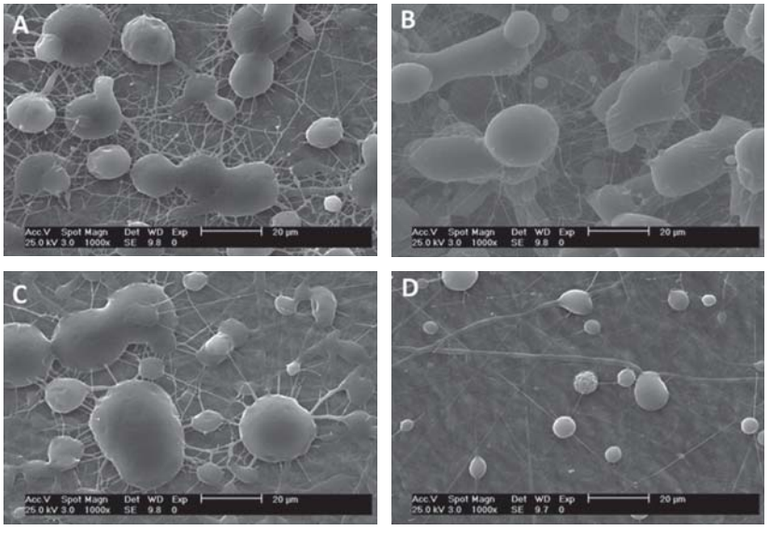

Figure 8 SEM images of PU electrospun fibers **A**) S16, **B**) S17, **C**) S18 y and **D**) S19.

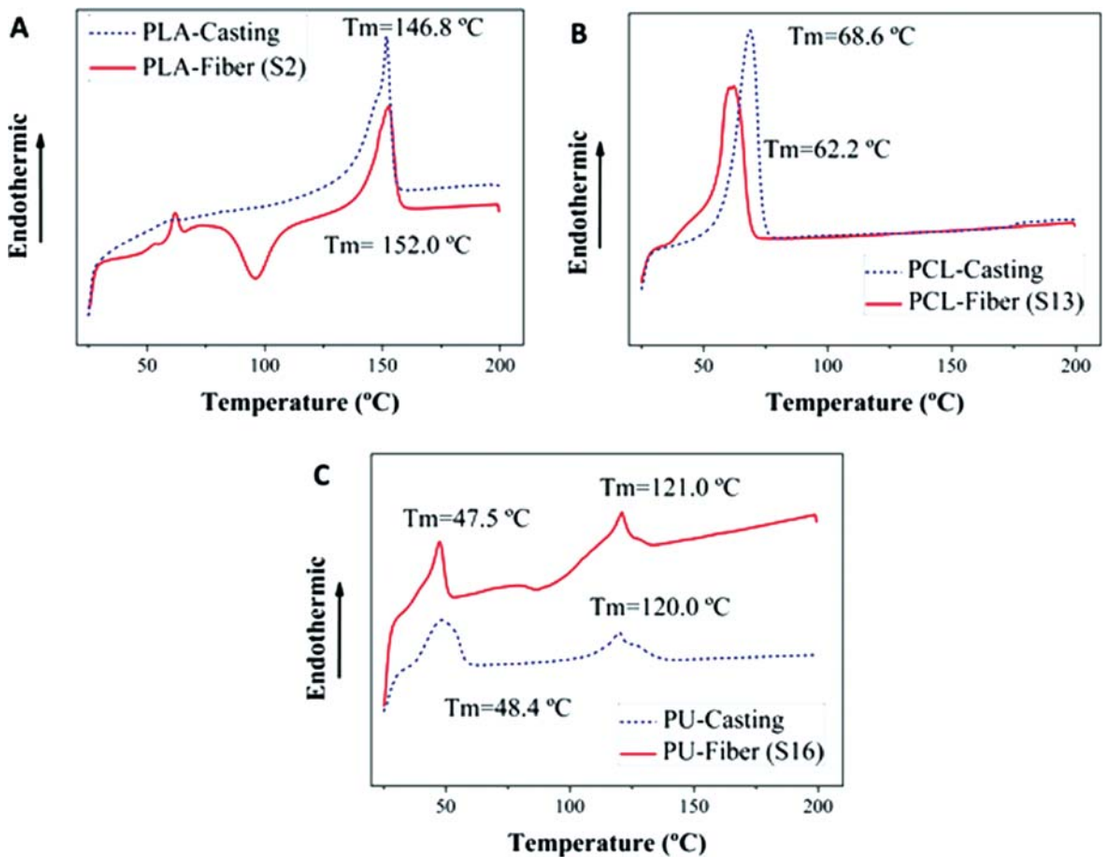

Figure 9 Comparative DSC heating scan curves of films and fibers of **A**) PLA, **B**) PCL and **C**) PU.

Table 8 Main thermal characteristics for PLA, PCL and PU fibers and films.

Polymer	$T_{m, PLA}$ (°C)	$T_{g, PLA}$ (°C)	$\Delta H_{f, PLA}$ (J/g)	$X_{c,cool\ PLA}$ (%)	$X_{c, PLA}$ (%)	$T_{m, PCL}$ (°C)	$T_{g, PCL}$ (°C)	$\Delta H_{f, PCL}$ (J/g)	$X_{c, PCL}$ (%)	$X_{c, PU}$ (%)	$T_{g, PU}$ (°C)
PLA film	153.4	56.7	37.2	–	40	–	–	–	–	–	–
PLA-S2	152.0	56.7	19.9	19.2	2.1	–	–	–	–	–	–
PCL film	–	–	–	–	–	66.4	–60.6	76.3	51.5	–	–
PCL-S13	–	–	–	–	–	62.2	–63.0	59.2	40.0	–	–
PU film	120.0	–	15.3	–	16.4	48.3		21.4	14.4	15.4	–31.6
PU-S16	121.0	–	27.0	–	29.0	47.4		13.3	8.9	19.0	–29.2

of the solvent can reduce the mobility of the polymer and so its ability for crystallinity arrangements [5]. On the other, the alignment of the polymeric chains can promote the crystallization.

In the case of PLA electrospun fibers, a small endothermic peak at about 60°C indicates the evaporation of chloroform. This fact indicates the presence of residual solvent in the electrospun fibers, as the chloroform boiling point is about 62°C [1]. Moreover, cold crystallization during sample heating is observed as a consequence of the rapid solvent evaporation during the electrospinning process that leads to quenching conditions and to the formation of nonhomogeneous PLA crystals along the electrospun fibers, changing the amorphous/crystalline nature of them compared with the polymer-casting film.

The PU crystallization has been calculated keeping the composition in mind and considering that the initial tri-block composition ratio between PLA and PCL is 50:50 in weight.

In general, when both PCL and PLA are able to crystallize, the degree of crystallization of PCL is higher than PLA [31]. In our case, PLA and PCL electrospun fibers show lower crystallinity degree than the corresponding solvent-casting films. In general, as expected, the crystallinity of PLA fibers is lower than that of PCL fibers. Moreover, PCL electrospun fibers show a lower degree of crystallization than their corresponding solvent-casting films. So, in conclusion, for both PCL and PLA, the crystallization process is more affected by solvent evaporation than by chain alignment effects. In fact, the fast solvent evaporation reduces the mobility of the polymeric chains during the solidification process, decreasing the degree of crystallinity in the electrospun fibers with respect to the respective casting-films.

The case of PU is different. In fact, the degree of crystallization for the PU electrospun fiber is higher than the one obtained for its film, due to the alignment of the polymeric chains produced by the stretching during the electrospinning process favoring the crystallization process. But it is important to note that, when analyzing the degree of crystallization for each block, in the case of PLA block, the crystallization is promoted by the electrospinning process but the crystallization of the PCL block in the electrospun fibers is unfavored. This fact can be related to the presence of the PLA crystals that can strongly influence and impede the crystallization of PCL in the block copolymer, as reported by us in our previous research [32].

4 CONCLUSIONS

Electrospun fibers of PLA, PCL and PU have been obtained by the electrospinning process. Optimum concentration is defined as the minimum concentration to obtain bead-free fibers with the smallest possible diameter. When higher polymer concentrations are employed to prepare electrospun fibers, the size of the fibers' diameters increase. On the other hand, an increment of polymer concentration provides higher polymer solution viscosity, which causes fluctuations of polymer solution flow, obtaining beads on fibers.

Bead-free fibers can be obtained by applying high voltages, which produce a greater elongation of the polymeric particles due to an increment of Coulomb forces. In addition, lower polymer and solvent solution flow-rates produce electrospun fibers with lower diameters, thus providing a faster solvent evaporation.

Finally, the crystallization behavior of electrospun fibers has been compared with the solvent-casting films of the same polymers. In particular, in the case of PLA and PCL, electrospun fibers show a lower crystallinity degree than the corresponding films due to the fast solvent evaporation, which produces a decrement on the mobility of the polymeric chains during the solidification process. However, in the case of PU, a higher crystallization has been observed in the fibers, which is the consequence of the fibers stretching and the chain alignment in the electrospinning process.

ACKNOWLEDGMENTS

We are indebted to the Spanish Ministry of Science and Innovation (MICINN) for their economic support of this research (MAT2010-21494-C03-03). LP also acknowledges the support of a JAE-DOC grant from CSIC cofinanced by the FSE.

REFERENCES

1. D. Garlotta, A literature review of poly(lactic acid). *J. Polym. Environ.* **9**, 63–84 (2002).
2. J. Lunt, Large-scale production, properties and commercial applications of polylactic acid polymers. *Polym. Degrad. Stab.* **59**, 145–152 (1998).
3. V.P. Martino, R.A. Ruseckaite, and A. Jimenez, Thermal and mechanical characterization of plasticized poly(l-lactide-co-d,l-lactide) films for food packaging. *J. Therm. Anal. Calorim.* **86**, 707–712 (2006).
4. M.A. Woodruff and D.W. Hutmacher, The return of a forgotten polymer—Polycaprolactone in the 21st century. *Prog. Polym. Sci.* **35**, 1217–1256 (2010).
5. N. López-Rodríguez, A. López-Arraiza, E. Meaurio, and J.R. Sarasua, Crystallization, morphology, and mechanical behavior of polylactide/poly(ε-caprolactone) blends. *Polym. Eng. Sci.* **46**, 1299–1308 (2006).
6. L. Li, H. Li, Y. Qian, X. Li, G.K. Singh, L. Zhong, W. Liu, Y. Lv, K. Cai, and L. Yang, Electrospun poly(varepsilon-caprolactone)/silk fibroin core-sheath nanofibers and their potential applications in tissue engineering and drug release. *Int. J. Biol. Macromol.* **49**, 223–232 (2011).
7. I. Navarro-Baena, A. Marcos-Fernandez, A. Fernandez-Torres, J.M. Kenny, and L. Peponi, Synthesis of PLLA-b-PCL-b-PLLA linear tri-block copolymers and their corresponding poly(esterurethane)s: Effect of the molecular weight on their crystallisation and mechanical properties. *RSC Adv.* **4**, 8510–8524 (2014).
8. O. Jeon, S.-H. Lee, S.H. Kim, Y.M. Lee, and Y.H. Kim, Synthesis and characterization of poly(l-lactide)−poly(ε-caprolactone) multiblock copolymers. *Macromolecules* **36**, 5585–5592 (2003).
9. L. Peponi, A. Marcos-Fernandez, and J.M. Kenny, Nanostructured morphology of a random

P(DLLA-co-CL) copolymer. *Nanoscale Res. Lett*. **7**, 103 (2012).
10. L. Peponi, I. Navarro-Baena, A. Sonseca, E. Gimenez, A. Marcos-Fernandez, and J.M. Kenny, Synthesis and characterization of PCL–PLLA polyurethane with shape memory behavior. *Eur. Polym. J.* **49**, 893–903 (2013).
11. G.-Y. Liao, L. Chen, X.-Y. Zeng, X.-P. Zhou, X.-L. Xie, E.J. Peng, Z.-Q. Ye, and Y.-W. Mai, Electrospun poly(l-lactide)/poly(ε-caprolactone) blend fibers and their cellular response to adipose-derived stem cells. *J. Appl. Polym. Sci.* **120**, 2154–2165 (2011).
12. A. Pedicini and R.J. Farris, Mechanical behavior of electrospun polyurethane. *Polymer* **44**, 6857–6862 (2003).
13. M.S. Khil, D.I. Cha, H.Y. Kim, I.S. Kim, and N. Bhattarai, Electrospun nanofibrous polyurethane membrane as wound dressing. *J. Biomed. Mater. Res. Part B Appl. Biomater*. **67B**, 675–679 (2003).
14. M.Ö. Seydibeyoğlu, M. Misra, A. Mohanty, J.J. Blaker, K.-Y. Lee, A. Bismarck, and M. Kazemizadeh, Green polyurethane nanocomposites from soy polyol and bacterial cellulose. *J. Mat. Sci.* **48**, 2167–2175 (2012).
15. S.Y. Chew, Y. Wen, Y. Dzenis, and K.W. Leong, The role of electrospinning in the emerging field of nanomedicine. *Curr. Pharm. Des.* **12**, 4751–4770 (2006).
16. F. Mei, J. Zhong, X. Yang, X. Ouyang, S. Zhang, X. Hu, Q. Ma, J. Lu, S. Ryu, and X. Deng, Improved biological characteristics of poly(l-lactic acid) electrospun membrane by incorporation of multiwalled carbon nanotubes/hydroxyapatite nanoparticles. *Biomacromolecules* **8**, 3729–3735 (2007).
17. S. Mojtaba Alizadeh Darbandi, M. Nouri, and J. Mokhtari, Electrospun nanostructures based on polyurethane/MWCNTs for strain sensing applications. *Fibers Polym.* **13**, 1126–1131 (2012).
18. C. Yang, X. Wu, Y. Zhao, L. Xu, and S. Wei, Nanofibrous scaffold prepared by electrospinning of poly(vinyl alcohol)/gelatin aqueous solutions. *J. Appl. Polym. Sci.* **121**, 3047–3055 (2011).
19. Z.-M. Huang, Y.Z. Zhang, M. Kotaki, and S. Ramakrishna, A review on polymer nanofibers by electrospinning and their applications in nanocomposites. *Compos. Sci. Technol.* **63**, 2223–2253 (2003).
20. N. Amiraliyan, M. Nouri, and M.H. Kish, Effects of some electrospinning parameters on morphology of natural silk-based nanofibers. *J. Appl. Polym. Sci.* **113**, 226–234 (2009).
21. H. Zhou, T.B. Green, and Y.L. Joo, The thermal effects on electrospinning of polylactic acid melts. *Polymer* **47**, 7497–7505 (2006).
22. A. Sonseca, L. Peponi, O. Sahuquillo, J.M. Kenny, and E. Giménez, Electrospinning of biodegradable polylactide/hydroxyapatite nanofibers: Study on the morphology, crystallinity structure and thermal stability. *Polym. Degrad. Stab.* **97**, 2052–2059 (2012).
23. M. Bognitzki, T. Frese, M. Steinhart, A. Greiner, J.H. Wendorff, A. Schaper, and M. Hellwig, Preparation of fibers with nanoscaled morphologies: Electrospinning of polymer blends. *Polym. Eng. Sci.* **41**, 982–989 (2001).
24. S.H. Tan, R. Inai, M. Kotaki, and S. Ramakrishna, Systematic parameter study for ultra-fine fiber fabrication via electrospinning process. *Polymer* **46**, 6128–6134 (2005).
25. S.K. Tiwari, and S.S. Venkatraman, Importance of viscosity parameters in electrospinning: Of monolithic and core–shell fibers. *Mater. Sci. Eng. C* **32**, 1037–1042 (2012).
26. C.-M. Wu, H.-G. Chiou, S.-L. Lin, and J.-M. Lin, Effects of electrostatic polarity and the types of electrical charging on electrospinning behavior. *J. Appl. Polym. Sci.* **126**, E89-E97 (2012).
27. V. Jacobs, R.D. Anandjiwala, and M. Maaza, The influence of electrospinning parameters on the structural morphology and diameter of electrospun nanofibers. *J. Appl. Polym. Sci.* **115**, 3130–3136 (2010).
28. A. Greiner and J.H. Wendorff, Electrospinning: A fascinating method for the preparation of ultrathin fibers. *Angew. Chem. Int. Ed. Engl.* **46**, 5670–5703 (2007).
29. D.W. Van Krevelen: *Properties of Polymers*, 3rd ed. pp. 120–123, Elsevier Science B.V., Amsterdam. (1990).
30. S. Pensec, M. Leroy, H. Akkouche, and N. Spassky, Stereocomplex formation in enantiomeric diblock and triblock copolymers of poly (ε-caprolactone) and polylactide. *Polym. Bull.* **45**, 373–380 (2000).
31. I.W. Hamley, V. Castelletto, R.V. Castillo, A.J. Müller, C.M. Martin, E. Pollet, and Ph. Dubois, Crystallization in poly(l-lactide)-b-poly(ε-caprolactone) double crystalline diblock copolymers: A study using x-ray scattering, differential scanning calorimetry, and polarized optical microscopy. *Macromolecules* **38**, 463–472 (2005).
32. L. Peponi, I. Navarro-Baena, J.E. Báez, J.M. Kenny, and A. Marcos-Fernández, Effect of the molecular weight on the crystallinity of PCL-b-PLLA di-block copolymers. *Polymer* **53**, 4561–4568 (2012).